

## Reduction of etching plasma damage on low dielectric constant fluorinated amorphous carbon films by multiple H<sub>2</sub> plasma treatment

Jia-Min Shieh, Kou-Chiang Tsai, Bau-Tong Dai, Yew-Chung Wu, and Yu-Hen Wu

Citation: *Journal of Vacuum Science & Technology B* **20**, 1476 (2002); doi: 10.1116/1.1494067

View online: <http://dx.doi.org/10.1116/1.1494067>

View Table of Contents: <http://scitation.aip.org/content/avs/journal/jvstb/20/4?ver=pdfcov>

Published by the AVS: Science & Technology of Materials, Interfaces, and Processing

---

### Articles you may be interested in

[In situ x-ray photoelectron spectroscopy analysis of SiO<sub>x</sub>F<sub>y</sub> passivation layer obtained in a SF<sub>6</sub>/O<sub>2</sub> cryoetching process](#)

*Appl. Phys. Lett.* **94**, 071501 (2009); 10.1063/1.3085957

[Role of fluorine in plasma nitridated ZrO<sub>2</sub> thin films under irradiation](#)

*Appl. Phys. Lett.* **93**, 122907 (2008); 10.1063/1.2991445

[Effects of fluorine incorporation and forming gas annealing on high- \$k\$  gated germanium metal-oxide-semiconductor with GeO<sub>2</sub> surface passivation](#)

*Appl. Phys. Lett.* **93**, 073504 (2008); 10.1063/1.2966367

[Fluorine effects on the dipole structures of the Al<sub>2</sub>O<sub>3</sub> thin films and characterization by spectroscopic ellipsometry](#)

*Appl. Phys. Lett.* **90**, 172904 (2007); 10.1063/1.2730581

[In situ real-time monitoring of profile evolution during plasma etching of mesoporous low-dielectric-constant SiO<sub>2</sub>](#)

*J. Vac. Sci. Technol. A* **23**, 347 (2005); 10.1116/1.1865154

---



## Re-register for Table of Content Alerts

Create a profile.



Sign up today!



# Reduction of etching plasma damage on low dielectric constant fluorinated amorphous carbon films by multiple H<sub>2</sub> plasma treatment

Jia-Min Shieh,<sup>a)</sup> Kou-Chiang Tsai, and Bau-Tong Dai  
*National Nano Device Laboratories, Hsinchu 30050, Taiwan*

Yew-Chung Wu and Yu-Hen Wu  
*Institute of Materials Science and Engineering, National Chiao Tung University, Hsinchu 30050, Taiwan*

(Received 20 March 2002; accepted 20 May 2002)

Two-step hydrogen plasma treatment on low dielectric constant (low-*k*) fluorinated amorphous carbon films (*a*-C:F) was conducted to improve their thermal stability and reduce the damage caused by the patterning processes. First, hydrogen plasma treatment repairs imperfect bonds of as-deposited *a*-C:F films, stabilizing their chemical structures and increasing their resistance against elevated thermal stresses. After this passivation process, an additional hydrogen plasma treatment was applied to *a*-C:F films that had been etched using a mixture of N<sub>2</sub>+O<sub>2</sub>+CHF<sub>3</sub>, enabling sub-130 nm damascene trenches to be patterned and repairing the chemical structures destroyed by the etching plasma. © 2002 American Vacuum Society. [DOI: 10.1116/1.1494067]

## I. INTRODUCTION

Low dielectric constant (low-*k*) materials as interlayer dielectrics face similar difficulties, whether deposited by chemical vapor deposition (CVD) or by spin-on techniques.<sup>1</sup> These difficulties include integration issues,<sup>2</sup> weak resistance against copper diffusion,<sup>3</sup> and the avoidance of damage during patterning.<sup>4</sup> Low-*k* materials such as black diamond SiOC:H films<sup>5</sup> and fluorinated amorphous carbon (*a*-C:F) films<sup>6</sup> are increasingly attracting interest since they can be deposited by conventional plasma-enhanced CVD (PECVD). The gaseous mixture, containing fluorocarbon and hydrocarbon, is a precursor in the deposition of *a*-C:F films,<sup>6</sup> making the deposition of *a*-C:F films as easy as preparing fluorinated SiO<sub>2</sub> (SiOF) films. Several attempts have been made to address and improve critical areas of material properties of *a*-C:F films in interconnect processes.<sup>6–11</sup> However, Han and Bae reported that the electrical characteristics of *a*-C:F films become degraded after annealing at several hundred degrees, typically about 400 °C.<sup>7</sup>

Previous studies have demonstrated that plasma posttreatment is an effective means of modifying as-deposited dielectric films.<sup>12–15</sup> Hydrogen plasma treatment can normally repair unstable bonds, or defect sites, into stronger chemical structures.<sup>12–14</sup> The treated films were more resistant to moisture uptake and copper diffusion than untreated films.<sup>13,14</sup> Furthermore, the patterning process for low-*k* materials typically includes oxygen in the etching gases. However, oxygen gas attacks the low-*k* materials by decomposing chemical structures and generating unstable bonds in the films, increasing the probability of moisture uptake,<sup>15</sup> and thereby degrading the performance of low-*k* materials, such as *a*-C:F films.

This study demonstrates, for the first time, a multiple plasma treatment on *a*-C:F films. In the first step, a hydrogen plasma treatment converts dangling bonds of as-deposited *a*-C:F films into chemical structures which are more stable under higher thermal stresses. After the hydrogen plasma-treated *a*-C:F films are etched, an additional hydrogen plasma treatment was again employed, leading to the repair of the bonds damaged by the patterning processes. Hydrogen atoms are known to be able to penetrate deeply into dielectric films and mend imperfect bonds. Consequently, hydrogen plasma pretreatment combined with post-treatment can protect low-*k* materials such as *a*-C:F films from thermal stresses, and protect against damage due to etching.

## II. EXPERIMENT

As-deposited *a*-C:F films were deposited by PECVD. The basic precursor gas was a mixture of CH<sub>4</sub>, C<sub>4</sub>F<sub>8</sub>. In this experiment, another class of samples was the H<sub>2</sub> plasma-treated *a*-C:F films. Table I-a lists the deposition<sup>10</sup> and post-deposition parameters. For simplicity, STD represents the as-deposited *a*-C:F films, whereas H-3, H-6, and H-9 represent as-deposited *a*-C:F films with 3, 6, and 9 min of H<sub>2</sub> plasma treatment, respectively. Thermal stability was then examined by curing those *a*-C:F films in a furnace at elevated temperatures for 30 min in N<sub>2</sub> ambient at a flow rate of 10 liter/min. Before and after each treatment, the Fourier-transform infrared (FTIR) absorption spectra of each film were examined to monitor structural changes. Secondary ion mass spectroscopy (SIMS) was performed to analyze hydrogen distributions in the *a*-C:F films. Thermal desorption spectroscopy (TDS) was used to measure the gas release (such as H<sub>2</sub>O) from the *a*-C:F films, to examine the effect of plasma treatment on resistance against moisture uptake. The electrical measurements were taken by metal-insulator-semiconductor capacitors. Two types of wafers were used to

<sup>a)</sup>Author to whom all correspondence should be addressed; electronic mail: jmshieh@ndl.gov.tw

TABLE I. (a) Deposition and postdeposition parameters. (b) Etching parameters.

(a)	Deposition parameter	Postdeposition parameter
Reactant gases	$C_xF_y/CH_4 \sim 10$	$NH_3, N_2,$ and $H_2$
rf plasma power	200 W	200 W
Process pressure	550 mTorr	100 mTorr
Temperature	250 °C	250 °C
Flow rate	300 sccm	200 sccm
(b)	Etching parameters for $a-C:F$	Etching parameters for $SiO_2$
Reactant gases	$N_2/O_2 \sim 80/20$ or (65/35)	$CHF_3/CF_4 \sim 5/95$
rf plasma power	2000 W	2000 W
Bias power	60–120 W	60 W
Process pressure	5 mTorr	5 mTorr
Temperature	60 °C	60 °C
Flow rate	100 sccm	100 sccm

evaluate etching characteristics such as damage due to etching. These wafers were blanket  $a-C:F$  films, and  $a-C:F$  films covered with 50 nm of  $SiO_2$  for patterning experiments. A 50 nm silicon oxide mask was patterned by electron-beam lithography (smallest feature resolution  $\sim 50$  nm). Both types of wafers were etched in a helicon-wave plasma etching process. Etching gases,  $N_2$  and  $O_2$  were used at a total flow rate of 100 sccm, with the addition of  $CHF_3$  to control the etching profiles. Table I(b) lists other etching parameters.

### III. RESULTS AND DISCUSSION

#### A. Fundamental characteristics and thermal stabilities of plasma-modified low- $k$ $a-C:F$ films

Figure 1(a) shows that the dielectric constant of  $a-C:F$  films increases from 2.35 to 3.7 as the annealing temperature increases to 450 °C. Consequently, a modification, such as plasma treatments of as-deposited  $a-C:F$  films, was required in addition to the optimization of deposition conditions.  $NH_3$  plasma treatment is not applicable to  $a-C:F$  films since its refractive index and thickness changed by more than 9% in a process time of 1.5 min, although  $NH_3$  plasma effectively modified many materials.<sup>15</sup> Therefore, hydrogen plasma treatment was adopted herein. Figures 1(a), and 1(b) show the dielectric constants and the leakage currents of  $a-C:F$  films treated by  $H_2$  plasma remain relatively unchanged, because the hydrogen plasma repairs the unstable bonds or defect sites into stable chemical bonds. The leakage currents and dielectric constants of  $H_2$ -treated films can be improved or at least maintained. Notably, stresses of the  $H_2$ -treated  $a-C:F$  films are maintained at the same level ( $\sim 10$  MPa) as those of untreated films, and FTIR spectra for the chemical structures of such films are also the same as those of the as-deposited samples, as shown in curve a and curve b of Fig. 2(a), implying that hydrogen plasma bombardment neither introduced a densification effect nor caused reconstruction in the  $a-C:F$  films. In general, some dangling bonds caused by deposition, thermal stresses, or patterning processes may temporarily exist on the surface of the film. Those unstable sites tend to react with other species (mois-

ture) from the environment, degrading the electrical characteristics (by forming  $C=O$  bonds). However, the degradation of electrical characteristics due to imperfect bonds can be decreased by forming stable bonding structures (hydrogen passivated bonds).

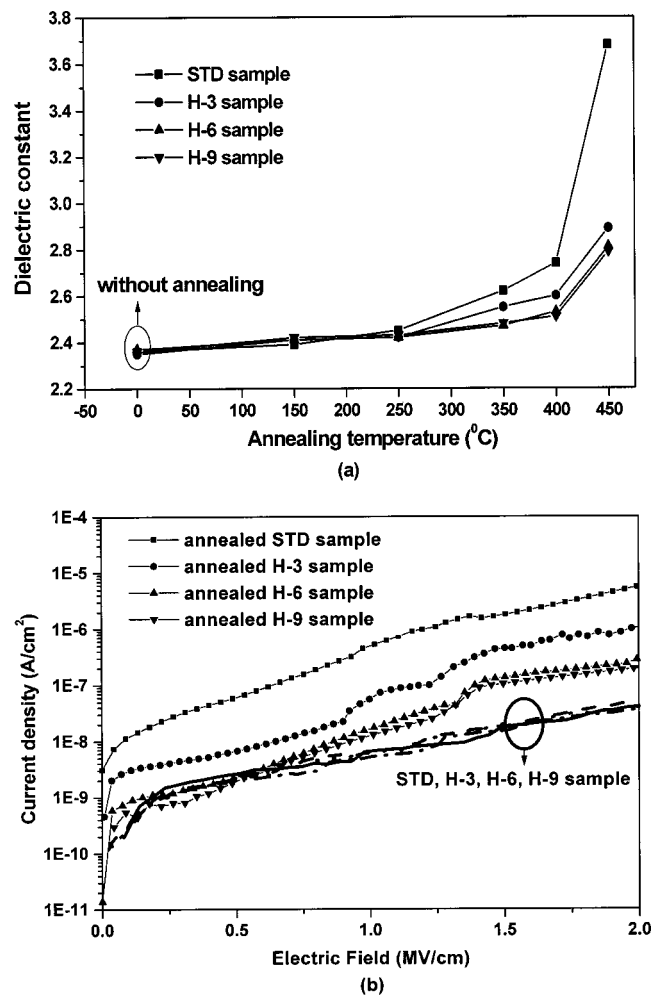


FIG. 1. (a) Dielectric constants of  $H_2$ -treated  $a-C:F$  films as functions of annealing temperature. (b) Leakage currents of STD samples,  $H_2$ -treated  $a-C:F$  films before, and after annealing for 30 min at 450 °C.

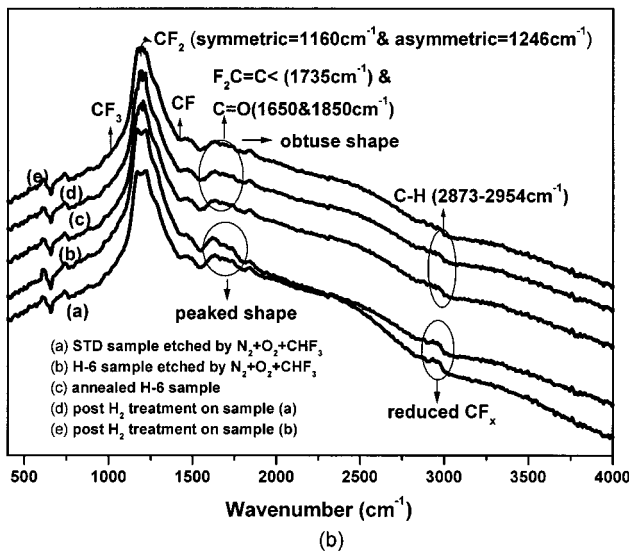
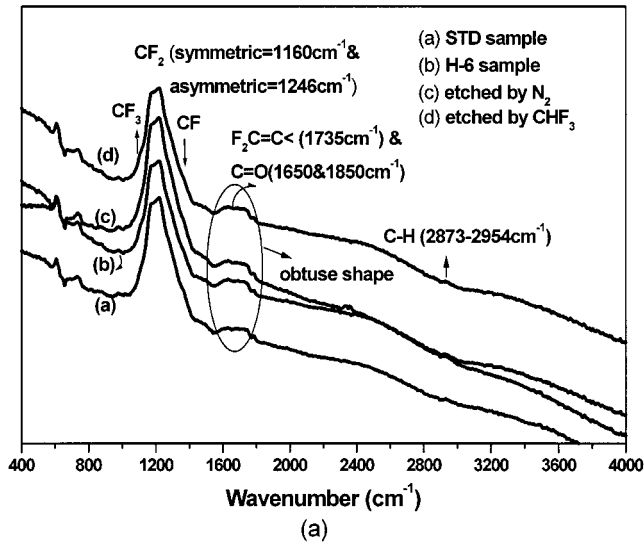


Fig. 2. (a) FTIR spectra of STD, H-6, and STD samples etched by N<sub>2</sub>, CHF<sub>3</sub>. (b) FTIR spectra of a-C:F films etched by N<sub>2</sub>+O<sub>2</sub>+CHF<sub>3</sub>; etched samples with post H<sub>2</sub> treatment, and annealed H-6 sample.

Figure 1 (a) displays the dielectric constants of H<sub>2</sub>-treated a-C:F films as a function of annealing temperature and illustrates that its dielectric constant rises from 2.35 to 2.8 as the annealing temperature increases to 450 °C. In comparison, the untreated sample abruptly changes its electrical characteristics, and its dielectric constant rises to 3.7 such that the thermal stability of the dielectric constants of a-C:F films is significantly improved after treatment with H<sub>2</sub> plasma. Moreover, strongly H<sub>2</sub>-passivated samples (H-6 and H-9) were more stable than other samples at all annealing temperatures. After thermal annealing at 450 °C for 30 min, the leakage currents of H-6 and H-9 samples were also much lower than those of H-3 and STD samples, as depicted in Fig. 1 (b). For example, the leakage current of H-6 and H-9 samples only increases from  $I_d \approx 6.0 \times 10^{-9}$  A/cm<sup>2</sup> to  $I_d \approx 1.28 \times 10^{-8}$  A/cm<sup>2</sup> (@  $E_{bias} = 1.0$  MV/cm) after thermal annealing at 450 °C. The values for annealed H-3 and STD

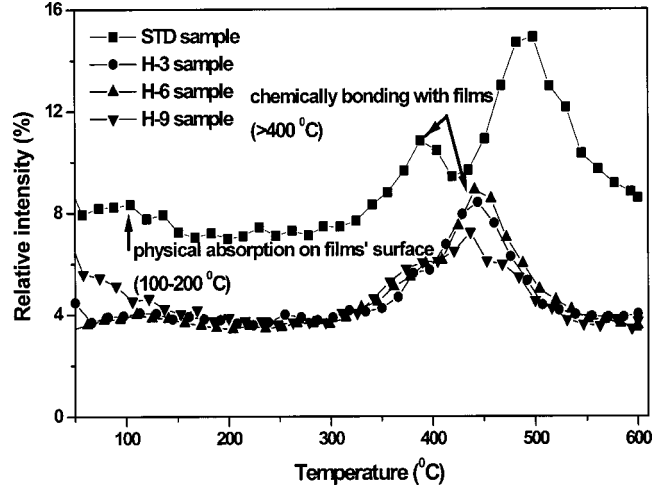


Fig. 3. TDS spectra of H<sub>2</sub>O desorption as a function of temperature for a-C:F films with H<sub>2</sub> treatments of 3, 6, and 9 min.

samples are  $I_d \approx 5.8 \times 10^{-8}$  A/cm<sup>2</sup> and  $I_d \approx 5.0 \times 10^{-7}$  A/cm<sup>2</sup>, respectively.

Therefore, hydrogen plasma treatment helps to stabilize the chemical structures of a-C:F films because of the presence of hydrogen passivated chemical structures in the films, which modification for H<sub>2</sub>-treated a-C:F films can suppress the uptake of moisture and reduce thermal decomposition during high-temperature annealing. Figure 3 displays TDS spectra that verify the presence of more hydrophobic surfaces in the H<sub>2</sub>-treated samples than in the other samples, and that the desorption amount of H<sub>2</sub>O of the H-9 sample is the least among all samples. In those TDS spectra, H<sub>2</sub>O physically absorbing on the surface of the film dominates the desorption in the lower temperature below 200 °C and H<sub>2</sub>O chemically bonding with films contributes the desorption in the higher temperature above 400 °C. Curve c in Fig. 2 (b) also shows that spectral peaks of CF<sub>x</sub>(980–1350 cm<sup>-1</sup>) and C—H (2873–2954 cm<sup>-1</sup>)<sup>11</sup> and the obtuse shape of the C=O bond in the FTIR spectrum of the annealed H-6 sample, are the same as those of the STD sample. However, Figs. 1 (a), 1 (b), and 3 reveal that the thermal stability of the H-9 sample was similar to that of the H-6 sample. An excess of hydrogen atoms in the H-9 sample might break the CF<sub>x</sub> bonds and actively react with fluorine species before outgassing via HF structures at elevated thermal stresses. This effect was the dominant reason for the saturation of treatment times. Considering the dielectric constants and leakage currents together, the H<sub>2</sub> treatment time of 6 min is enough to inhibit the degradation caused by thermal stresses.

**B. Hydrogen plasma treatments on etched a-C:F films**

Our previous work<sup>10</sup> demonstrated that a sidewall passivation, which is provided by nitrogen gas forming a C<sub>x</sub>N<sub>y</sub> layer, can help the N<sub>2</sub>/O<sub>2</sub> etching process to pattern a perfect 150 nm damascene structure on the a-C:F films. This study tries to improve the aspect ratios of the damascene trenches by increasing the bias power. Figure 4 (a) displays scanning

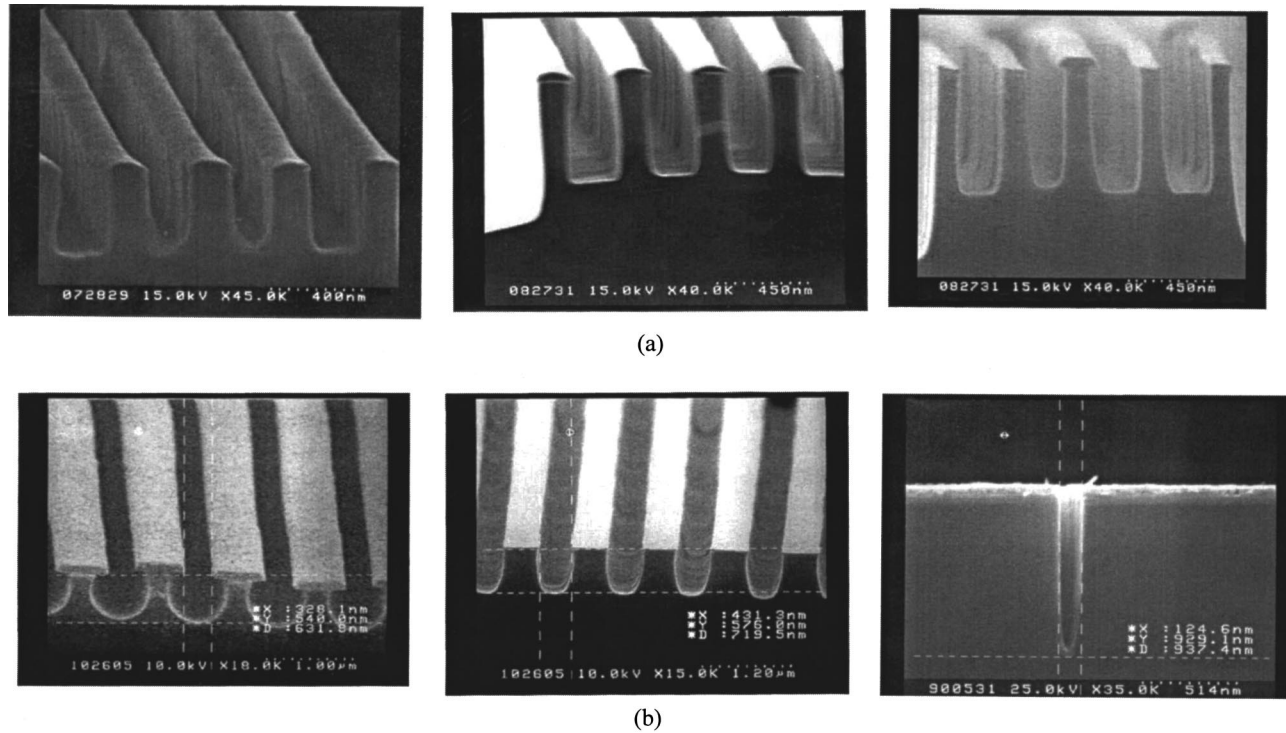


FIG. 4. (a) SEM profiles for patterned  $a$ -C:F films capped with 50 nm  $\text{SiO}_2$  as a hard mask for a range of bias power from 60 to 120 W. (b) left-hand side micrograph refers to the  $a$ -C:F film etched by the  $\text{N}_2/\text{O}_2$  recipe; central micrograph refers to the  $a$ -C:F films etched by the  $\text{N}_2/\text{O}_2/\text{CHF}_3$  recipe, and right-hand side micrograph refers to 130 nm damascene trenches patterned by  $\text{N}_2/\text{O}_2/\text{CHF}_3$  etching gases.

electron microscopy (SEM) micrographs for patterned  $a$ -C:F films capped with 50 nm  $\text{SiO}_2$  as a hard mask, for various bias powers from 60 to 120 W. The process time was 60 s; the photoresist sizes defined by electron-beam lithography was 130 nm, and  $\text{N}_2/\text{O}_2$  (80/20) etching gases for  $a$ -C:F films were used. An  $\text{CHF}_3/\text{CF}_4$  (5/95) etching gas was used to etch the  $\text{SiO}_2$  hard mask and all other parameters were the same as those used for etching the  $a$ -C:F films. Although the aspect ratio of the patterned damascene trenches increased from 2.3 to 2.7 as the bias power increased from 60 W to 120 W, the width of the patterned damascene trenches also increased from 160 nm to 230 nm because the increased energy of ion bombardment energy provided insufficient anisotropy of the etching rate in the narrowed trenches/vias and a vertical etching profiles could thus not be maintained. According to this result, an additional etching gas,  $\text{CHF}_3$ , was added to control the etching profiles. Its effect was examined by comparing the etching pattern [left-hand side micrograph of Fig. 4 (b)] in the  $\text{N}_2/\text{O}_2$  process with that [central micrograph of Fig. 4 (b)] using the  $\text{N}_2/\text{O}_2/\text{CHF}_3$  recipe. The flow rate of the additional  $\text{CHF}_3$  gas was 10 sccm. A larger pattern of around 400 nm and an enhanced isotropic etching rate, obtained with a lower ratio of  $\text{N}_2/\text{O}_2$  (65/35), were employed to examine the contribution of  $\text{CHF}_3$  to the passivation of the sidewalls. The central micrograph of Fig. 4 (b) shows protection of the sidewall of the pattern was observed, and an excellent profile of 130 nm damascene trenches was patterned by the  $\text{N}_2/\text{O}_2/\text{CHF}_3$  etching gases, as shown in the right-hand side micrograph of Fig. 4 (b).

Except in the case of the control of the etching profile by etching recipes, attack by oxygen from the etching plasmas or photoresist stripping processes is a critical issue for low- $k$  materials. The FTIR spectra in curve c and curve d of Fig. 2 (a), shows that the  $\text{N}_2$  and  $\text{CHF}_3$  gases do not observably affect the chemical structures of  $a$ -C:F films. In comparison, oxygen gas apparently alters the characteristics of the film, as concluded from the appearance of enlarged C=O bonds ( $1650$  and  $1850\text{ cm}^{-1}$ ) in curve a and curve b of Fig. 2 (b).

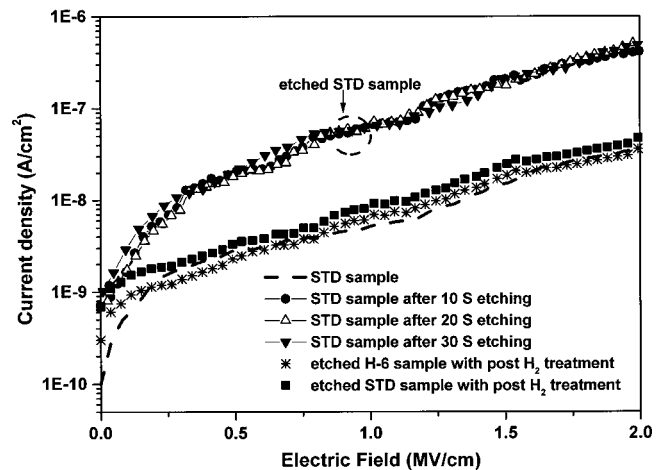


FIG. 5. Leakage currents of STD samples; STD samples etched for different process times; etched STD samples with post  $\text{H}_2$  treatment, and etched H-6 samples with post  $\text{H}_2$  treatment.

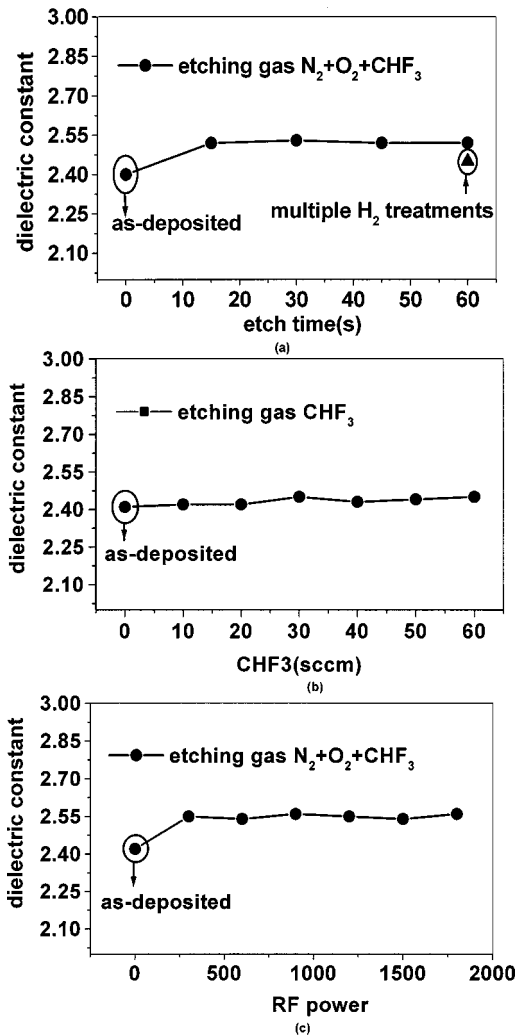


FIG. 6. (a) Dielectric constants for *a*-C:F films etched by  $N_2+O_2+CHF_3$  gases as functions of etching process times. (b) Dependence of the concentration of the  $CHF_3$  etching gas on dielectric constants of *a*-C:F films. (c) Dependence of the rf power on dielectric constants of *a*-C:F films etched by  $N_2+O_2+CHF_3$  gases.

These bonds differ from the obtuse shapes for STD or annealed H-6 samples. Damage caused by etching plasmas finally increased the leakage currents and dielectric constants of *a*-C:F films, as shown in Figs. 5 and 6(a). The mean leakage current increased from  $I_d \approx 6.0 \times 10^{-9}$  A/cm<sup>2</sup> to  $I_d \approx 7.0 \times 10^{-8}$  A/cm<sup>2</sup> ( $@E_{bias} = 1.0$  MV/cm) for *a*-C:F films after the etching processes, and the dielectric constant increased to  $\kappa \approx 2.55$  ( $\kappa \approx 2.35$  for as-deposited *a*-C:F films). Figure 6(b) also showed that the addition of  $CHF_3$  etching gas did not obviously change the dielectric constants of the etched *a*-C:F films. The dielectric constants of *a*-C:F films etched with different bias powers were  $\kappa \approx 2.55$ , as shown in Fig. 6(c). Thus, increasing the power seems not further to damage *a*-C:F films. Therefore, attack by oxygen is a major factor that determines the damage caused by etching. The oxygen plasma causes several functional groups ( $C-F_x$ ) to breakdown, not only replacing them with hydroxyl groups or absorbed water, but also leaving many dangling bonds in *a*-C:F films. Curve a and curve b in Fig. 2(b) show the

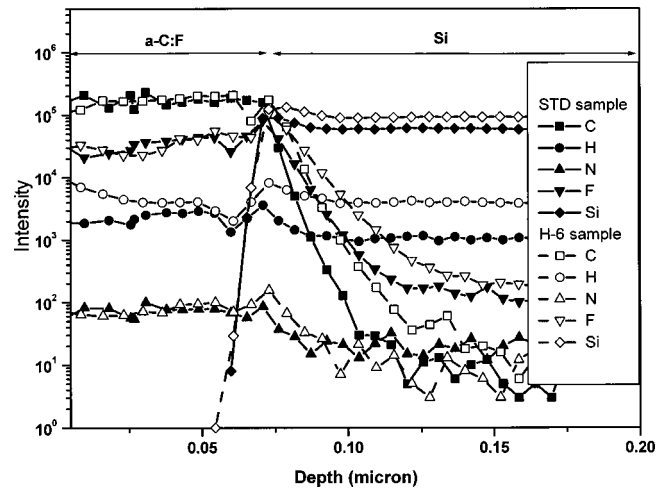


FIG. 7. Distribution profiles of hydrogen elements in  $H_2$ -treated *a*-C:F films analyzed by SIMS.

enlarged C=O and C—H bonds in the FTIR spectra of etched *a*-C:F films, indicating an uptake of moisture and chemical reconstruction in such films.

Therefore, in this study, posthydrogen plasma treatment was applied to the etched *a*-C:F films, and was expected to convert the damaged bonds into more stable chemical bonds. Curve d and curve e of Fig. 2(b) reveal that weaker C=O bonds were actually measured for etched *a*-C:F films with  $H_2$  posttreatments. The leakage currents of etched *a*-C:F samples with posttreatment were also found to be reduced to those of the STD samples, as shown in Fig. 5. Moreover, the etched samples with the two-step plasma treatments exhibited passivation superior to that of the etched STD sample with only a posttreatment, as determined by comparing their corresponding FTIR spectra and leakage currents. Oxygen plasma etches *a*-C:F films by chemical reactions, not only breaking the chemical bonds (i.e.,  $C-F_x$ ) but also replacing them with C=O bonds. These reactions occur on the surfaces and interiors of the film by the diffusion of oxygen radicals into the porous inner structure of *a*-C:F films to attack weakly bonded structures. The hydrogen in the H-6 sample penetrated deeply into *a*-C:F films as shown in SIMS analyses of Fig. 7, causing initial passivation of *a*-C:F films against sequential damage from etching plasmas, even when the outer portions of *a*-C:F films were removed during patterning processes. The electrical characteristics of *a*-C:F films with multiple  $H_2$  treatments improved after patterning.

#### IV. CONCLUSION

A novel two-step hydrogen plasma treatment was for the first time applied to low-*k* *a*-C:F films, to passivate the chemical structures against thermal stress, and attack by oxygen during patterning processes. First, the hydrogen plasma treatment increased the thermal stability of *a*-C:F films. Hydrogen elements penetrated deeply into *a*-C:F films, providing an initial passivation against sequential damage caused by etching plasmas. Further hydrogen treatment could repair the damage caused by the etching of  $H_2$ -treated *a*-C:F films.

## ACKNOWLEDGMENTS

The authors would like to thank the National Science Council of the Republic of China for financially supporting this research under Contract No. NSC91-2721-2317-200.

- <sup>1</sup>L. Peter, *Semicond. Int.* **64** (1998).
- <sup>2</sup>M. Hiroi, M. Tada, H. Ohtake, S. Saito, T. Onodera, N. Furutake, Y. Harada, Y. Hayashi, and S. Sagamihara, *IITC* **295** (2001).
- <sup>3</sup>A. L. S. Loke, J. T. Wetzell, P. H. Townsend, T. Tanabe, R. N. Vrtis, M. P. Zussman, D. Kumar, C. Ryu, and S. S. Wong, *IEEE Trans. Electron Devices* **46**, 2178 (1999).
- <sup>4</sup>M. Lepage, D. Shamiryan, M. Baklanov, H. Struyf, G. Mannaert, S. Vanhaelemeersch, K. Weidner, and H. Meynen, *IITC* **174** (2001).
- <sup>5</sup>B. K. Hwang, M. J. Loboda, G. A. Cerny, R. F. Schneider, J. A. Seifferly, and T. Washer, *IITC* **52** (2000).
- <sup>6</sup>K. Endo and T. Tatsumi, *Appl. Phys. Lett.* **68**, 2864 (1996).
- <sup>7</sup>S.-S. Han and B.-S. Bae, *J. Electrochem. Soc.* **148**, F67 (2001).
- <sup>8</sup>H. Yang, D. J. Tweet, Y. Ma, and T. Nguyen, *Appl. Phys. Lett.* **73**, 1514 (1998).
- <sup>9</sup>H. Yokomichi and A. Masuda, *J. Appl. Phys.* **86**, 2468 (1999).
- <sup>10</sup>J.-M. Shieh, S.-C. Suen, K.-C. Tsai, B.-T. Dai, Y.-C. Wu, and Y.-H. Wu, *J. Vac. Sci. Technol. B* **19**, 780 (2001).
- <sup>11</sup>I. Banerjee, M. Harker, L. Wong, P. A. Coon, and K. K. Gleason, *J. Electrochem. Soc.* **146**, 2219 (1999).
- <sup>12</sup>I. Wu, T. Huang, W. B. Jackson, A. G. Lewis, and A. Chiang, *IEEE Electron Device Lett.* **12**, 181 (1991).
- <sup>13</sup>Y. C. Quan, S. Yeo, C. Shim, J. Yang, and D. Jung, *J. Appl. Phys.* **89**, 1402 (2001).
- <sup>14</sup>T.-C. Chang, P.-T. Liu, Y.-J. Mei, Y.-S. Mor, T.-H. Perng, Y.-L. Yang, and S. M. Sze, *J. Vac. Sci. Technol. B* **17**, 2325 (1999).
- <sup>15</sup>P.-T. Liu, T.-C. Chang, H. Su, Y.-S. Mor, Y.-L. Yang, H. Chung, J. Hou, and S.-M. Sze, *J. Electrochem. Soc.* **148**, F30 (2001).